Journal Title
XX(X):2–18

DOI: 10.1177/ToBeAssigned
www.sagepub.com/
SAGE

Are higher gradient models capable of predicting the mechanical behavior also in case of wide-knit pantographic structures?

Mario Spagnuolo[1], M. Erden Yildizdag[1,2], Ugo Andreaus[3] and Antonio M. Cazzani[4]

Abstract

The central theme of this study is to investigate a remarkable capability of a second-gradient continuum model developed for pantographic structures. The model is applied to a particular type of this metamaterial, namely wide-knit pantograph. As the structure of this kind has low fiber density, applicability of such a continuum model may be questionable. To address this uncertainty, numerical simulations are conducted to analyze the behavior of a wide-knit pantographic structure, and the predicted results are compared with those measured experimentally under bias extension test. The results presented in this study show that the numerical predictions and experimental measurements are in good agreement, and therefore, in some useful circumstances, this model is applicable for the analysis of wide-knit pantographic structures.

Keywords

Mechanical metamaterials, pantographic structures, second-gradient modeling, additive manufacturing

Prepared using sagej.cls *[Version: 2017/01/17 v1.20]*

1 Introduction

Design of metamaterials has been of great interest to engineers and scientists due to the remarkable progress in additive manufacturing (AM) technologies in the last 20 years. Currently, with newly developed and improved techniques, fabrication of materials with complex microstructures exhibiting exotic and uncommon properties is not a far-fetched conception as before[1]. In this paper, we particularly focus on the behavior of pantographic structures – a type of mechanical metamaterial. In general, metamaterials are classified based on the main interaction phenomena occurring in their microstructures. A mechanical metamaterial, therefore, is a multi-scale structure whose overall response is related to mechanical interaction between lower scales constituting the hierarchical architecture of the material. We refer the reader to the extensive review paper of Barchiesi et al.[2] for state-of-the-art applications in the study of mechanical metamaterials.

A pantographic structure, corresponding to a real 3D-printed rectangular specimen as given in Fig. 1, consists of a planar grid constituted by two orthogonally oriented families of continuous fibers connected by pivots located at intersections. Due to their distinct properties, pantographic structures have been extensively investigated in the literature[3?] . From a purely theoretical point of view, the mechanical behavior of pantographic structures is an excellent example to prove the existence of higher-gradient continua, i.e, continua whose deformation energies depend on higher gradients of displacement field as opposed to the well-known Cauchy continuum where the deformation energy is only a function of the first gradient of displacement. On the other hand, from a practical point of view, pantographic structures can be subjected to large deformations remaining in elastic regime, which may be a promising feature in different applications.

Recent progress in manufacturing techniques have prompted the need for developing higher-gradient models as fabrication of materials with complex microstructures is becoming increasingly popular. Higher gradient modeling is actually not a new idea for mechanicians. In the history of mechanics, the roots of higher gradient modeling can be traced back to the impressive works presented by Italian mechanician Gabrio Piola in the mid-19th century[4–9]. Later, in the 20th century, higher gradient modeling was

[1]International Research Center for the Mathematics and Mechanics of Complex Systems, University of L'Aquila, Italy
[2]Department of Naval Architecture and Ocean Engineering, Istanbul Technical University, 34469, Maslak, Istanbul, Turkey
[3]Dipartimento di Ingegneria Strutturale e Geotecnica, UniversitÃ degli Studi di Roma "La Sapienza", Roma, Italy [4]Dipartimento di Ingegneria Civile, Ambientale e Architettura (DICAAR), UniversitÃ degli Studi di Cagliari, Italy

Corresponding author:
M. Erden Yildizdag
Email: yildizdag@itu.edu.tr

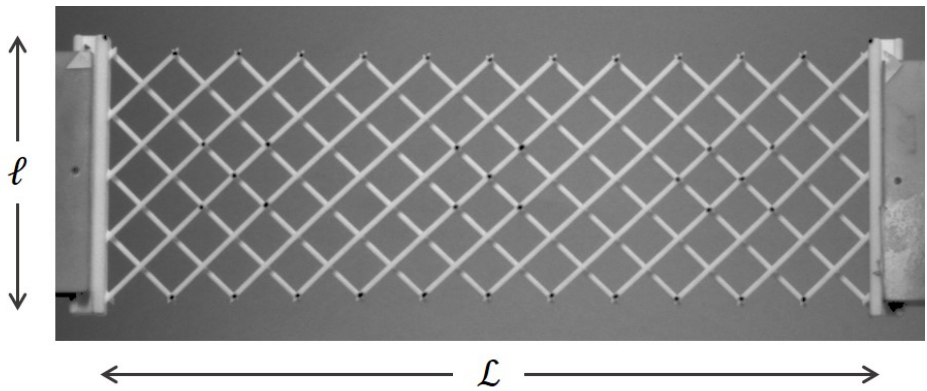

Figure 1. 3D-printed wide-knit pantographic structure composed by two families of fibers connected by pivots.

investigated and clearly formulated by different researchers. Here, we would especially like to mention two pioneering studies presented by Mindlin and Eshel[10] and Paul Germain[11]. In Mindlin and Eshel[10], the linear theory of elasticity was studied in the context of second gradient modeling, which the strain energy density depends on both the strain and its gradient. They studied the three different versions of strain energy density, providing the relation between those three different forms in terms of stress and boundary conditions. The differences between the strain energy densities come from the components included in the energy definitions. Importantly, to clarify the terminology, the term "second gradient" used in the present paper refers to the second gradient of displacement. As Mindlin and Eshel mentioned the first gradient of strain, the two terms "second gradient" and "first strain-gradient" are actually equivalent. Moreover, Mindlin and Eshel discussed how the angular moment balance equation cannot be derived directly by variational methods, and they rederived the complete equations starting from conservation laws (i.e. conservation of linear momentum, angular momentum and energy). Afterwards, Paul Germain[11] published another influential study on higher gradient modeling. The main idea of the paper is to show how variational methods can be systematically applied to study higher gradient theories. As Germain discussed in his paper, the variational methods provide a very effective and systematic way to obtain the required equations compared to other approaches followed in the past. Indeed, as discussed in many related studies[12,13], variational approaches are very powerful for mechanicians to establish new mathematical models quickly and efficiently. In this way, modern continuum mechanics applications can find more applications. In Germain[11], micromorphic media of order one were derived in detail, and subsequently, the equations for the general micromorphic medium were presented. For interested readers, we refer to Toupin[14], Eringen[15], Misra and Poorsolhjouy[16], Eremeyev[17] and Solyaev et al.[18] for further details.

Although promising theoretical effort was made on establishing higher gradient models, technology of that time was not sufficient to produce materials exhibiting such complex behaviors. Moreover, with increasing finite element method applications, the Cauchy continuum has been successfully applied in a large number of problems in various fields, and that is why scientists and engineers have disregarded higher gradient models for a long time. However, capabilities of advanced manufacturing techniques introduced in the last 20 years have clearly changed the opinions on developing higher gradient models.

This study focuses on the mechanical behavior of wide-knit pantographic structures. Pantographic structures have been extensively investigated in the recent literature (for instance, see [19–26]). A pantographic structure is referred to as *wide-knit* if the number of the fibers composing the grid is low. According to authors' best knowledge, this is the first study which investigates wide-knit pantographic structures as a second gradient continuum. In fact, in Andreaus et al.[27], this kind of structure has been studied by means of a meso-scale model, where the fibers composing the pantographic structure were modeled as Euler-Bernoulli nonlinear beams. We show a natural way to model the mechanical response of pantographic structures with a continuous second gradient model even when these structures are wide-knit, i.e. with fibers close enough to justify the use of a continuous theory (which, instead, is a logical choice when studying dense knitted fabrics). A fundamental point proposed in this article is to establish that the presence of some particular microstructures require the use of a second gradient theory to adequately describe the resulting material, even when the microstructure cannot actually be considered at a deeper scale of observation, as in the usual microstructured continua.

The organization of the paper is as follows: In Section 2, some important aspects of higher gradient modeling are remarked, and the model used in this study is summarized. Then, in Section 3, the theoretical predictions are presented and compared with experimental measures. Finally, in Section 4, we highlight our conclusions and try to provide some insights for future studies based on our observations.

2 Microstructure and Higher Gradient Theories

2.1 Microstructure induces higher gradient terms in equilibrium equations

Continuum Mechanics allows to study many "natural" materials accurately, approaching a huge number of problems with only few adjustments. Moreover, with the help of standard homogenization techniques, complex materials (e.g. composites) can be treated with the same tools used for homogeneous ones. Currently, due to the massive developments in computer technology and programming, it is possible to study with very complex problems. Modeling methods like the Finite Elements reduce the complexity of the problem to a mere question of number of degrees of freedom. In fact, it is always possible to introduce a mesh, as accurate as it is needed, to divide the considered medium in a certain number of, namely, finite elements with simple geometry, and then it is an easy task to solve the equations of the Continuum Mechanics. The more complex is

the geometry of the medium, the finer will be the required computational mesh, and therefore, a greater number of finite elements, thus increasing the number of degrees of freedom (i.e. of equations to be solved by the simulation tool). Despite the introduction of such tools, in some cases, the solution may require heavy numerical computation. For instance, media with complex geometries such as structures composed of bars or fibers: accurately describing such structures requires meshes with a huge number of finite elements. It has already been mentioned that classical homogenization techniques make it possible to overlook the problem of composites, reducing them to equivalent materials that globally have the same mechanical responses as the composite.

In the 1960s and 1970s, the problem of medium with microstructure was addressed by R. D. Mindlin, R. A. Toupin, and P. Germain in a number of papers. In their studies, different points of view of higher gradient modeling have been discussed to deal with materials equipped with microstructure, and they have shown how the existence of microstructure in some cases could induce higher order terms in the equilibrium equations of the material under consideration. Differently from classical homogenization techniques, in this case, equations containing terms dependent on second or higher order derivatives of displacement are obtained, inducing so-called higher gradient theory. Why do we pursue this way of thinking rather than trying to employ standard homogenization methods, for example, for composites? Our answer is very simple: the path followed by Mindlin, Toupin and Germain is effective and straightforward as the Principle of Virtual Works (or, equivalently, the Principle of Virtual Powers) is employed.

2.2 Variational principles in presence of microstructure

The Principle of Virtual Works (PVW) can be used systematically to deduce the fundamental equations for a given theory in Continuum Mechanics. As we have mentioned, there are multiple approaches that one can use to address the description of continua and find the governing equations, but the PVW provides the fastest way to get the sought equations and prevents errors that, in other approaches, might be difficult to detect.

As it was shown in Germain[11], when considering the problem of microstructured continua (also called micromorphic in Eringen's approach) the PVW provides equations of second gradient theories. Germain[11] shows that, by applying the Virtual Powers Principle (where virtual velocities are involved), the classical equations of the Continuum Mechanics are easily obtained. Here, the crucial point is to assign the right kinematics. Therefore, in case of a usual continuum, this is considered to be composed of a continuous distribution of particles which are geometrically represented by a material point M and by its velocity components U_i. When considering the microstructure, from a macroscopic point of view each particle is still represented by a material point M, but its kinematics must be defined more precisely. Germain gives a very clear and simple explanation of the relationship between kinematics, Principle of Virtual Powers and continuum theory. The main feature of the method explained in Germain[11] is that, assigned the required kinematics, the associated continuum theory can be deduced immediately via the PVW (or PVP). This is the fundamental reason why this method

is simpler than others proposed in the literature: it all reduces to the search for the kinematics associated with the studied problem.

2.3 Kinematics for the second gradient theory

Following the work of Germain[11], it can be shown how the kinematics due to the presence of the microstructure generates a second gradient continuum at macroscopic level. As mentioned earlier, in the classical description, a continuum consists of continuous distribution of particles, geometrically described by a point M and characterized by a velocity field, defined by its components U_i. However, in a theory which takes into account the presence of microstructure, each particle represented by a point M must be characterized by a more refined kinematics. Then, how do we describe the presence of microstructure from the kinematics point of view? At this stage, it is necessary to consider the continuum at microscopic level: each particle has to be considered as a continuum $P(M)$ of small extension. Germain shows in detail how the previous assumption implies that the velocity field U_i associated with the continuum $P(M)$ and the χ_{ij} field of the relative velocity gradients (resulting in a second order tensor) have to be considered. This final result makes it necessary to introduce the second gradient of the relative velocities x_{ijk}, which is a third order tensor. Therefore, it is clearly shown that the presence of a microstructure can be naturally described by introducing higher order terms in the continuum theory considered. This is the starting point in the study of pantographic structures. A certain microstructure is chosen in order to have a second gradient continuum as simple as possible and then homogenization techniques are utilized to determine an appropriate continuum model.

2.4 A second-gradient homogenized model

In dell'Isola et al.[20], it has been shown how to obtain a macroscopic second-gradient continuum model with a heuristic homogenization process which specifically consists in performing an identification procedure of macro-deformation energy which is associated to a postulated micro-model. Therefore, the macroscopic Lagrangian (line or surface) density of macro-deformation energy is obtained in terms of constitutive parameters appearing in the postulated expression of micro-deformation energy. Although the validity of the model presented by dell'Isola et al.[20] has been shown in different studies (see for example[28–34]) to predict the mechanical behavior of pantographic metamaterials, experimental evidences have shown that further improvements are unavoidable to establish a more robust model. Therefore, in this study, an improved model presented by Spagnuolo et al.[35] is adopted for the numerical simulations. In the study[35], the proposed improved model takes into account that the two families of fibers constituting the structure may not follow a single placement field description, as it was presented in dell'Isola et al.[20], due to the resistive behavior of pivots. Therefore, the strain energy of the model was formulated based on two *independent* placement fields to allow relative displacement between the two families of fibers.

If we assume a 2D continuum whose reference configuration is given by a rectangular domain $\Omega = [0, \mathcal{L}_1] \times [0, \mathcal{L}_2] \subset R^2$ (for example, in Fig. 1, $\mathcal{L}_1 = \mathcal{L}$ and $\mathcal{L}_2 = \ell$

represent the lengths of the sides of the ideal rectangle containing the pantographic structure) and by assuming that deformations are planar, the current configuration of Ω is described by the planar macro-placements $\boldsymbol{\chi}^1$ and $\boldsymbol{\chi}^2$ for each fiber family, respectively. Let be $\{\mathbf{D_1}, \mathbf{D_2}\}$ an orthogonal basis for the reference configuration. By following Spagnuolo et al.[35], the following strain energy is adopted in the numerical simulations

$$W(\varepsilon_\alpha, \kappa_\alpha, \gamma, \boldsymbol{\chi}^1, \boldsymbol{\chi}^2) = \sum_{\alpha=1}^{2} \left(\frac{1}{2} K_e^\alpha \varepsilon_\alpha^2 + \frac{1}{2} K_b^\alpha \kappa_\alpha^2 \right) + \frac{1}{2} K_p \gamma^2 + \frac{1}{2} K_f \|\boldsymbol{\chi}^1 - \boldsymbol{\chi}^2\|^2 \tag{1}$$

where ε_α is the stretch of fibers

$$\varepsilon_\alpha = \|\mathbf{F}^\alpha \mathbf{D}_\alpha\| - 1, \tag{2}$$

κ_α is the fiber curvature

$$\kappa_\alpha = \|\mathbf{c}_\alpha - (\mathbf{d}_\alpha \cdot \mathbf{c}_\alpha)\, \mathbf{d}_\alpha\| = \|(\mathbf{I} - \mathbf{d}_\alpha \otimes \mathbf{d}_\alpha)\, \mathbf{c}_\alpha\| \tag{3}$$

and γ denotes the shear distortion related to the angle change between fibers

$$\gamma = \left| \cos^{-1}(\mathbf{d}_1 \cdot \mathbf{d}_2) - \frac{\pi}{2} \right|. \tag{4}$$

Here, $\mathbf{c}_\alpha$ is an auxiliary vector field,

$$\mathbf{c}_\alpha = \frac{\nabla \mathbf{F}^\alpha \, (\mathbf{D}_\alpha \otimes \mathbf{D}_\alpha)}{\|\mathbf{F}^\alpha \mathbf{D}_\alpha\|} \tag{5}$$

and $\mathbf{d}_\alpha$ is the unit vectors tangent to each fiber family in the current configuration

$$\mathbf{d}_\alpha = \frac{\mathbf{F}^\alpha \mathbf{D}_\alpha}{\|\mathbf{F}^\alpha \mathbf{D}_\alpha\|} \tag{6}$$

where $\mathbf{F}^\alpha$ is the deformation gradient for each independent placement, $\mathbf{F}^\alpha = \nabla \boldsymbol{\chi}^\alpha$ (no summation over α). The terms K_e, K_b, K_p, and K_f are the constant and positive material parameters related to stretching, bending, shearing, and fiber connectivity, respectively.

Finally, the governing equations are obtained by the variational statement

$$\delta \int_\Omega W(\varepsilon_\alpha, \kappa_\alpha, \gamma, \boldsymbol{\chi}^1, \boldsymbol{\chi}^2)\, d\Omega = 0 \qquad \forall \delta \mathbf{u} \tag{7}$$

where $\delta \mathbf{u}$ belongs to the vector space of admissible displacement variations, i.e. test functions. In this study, as deformation is assumed to be quasi-static, kinetic energy is not included in the expression given in Eq. 7.

Additionally, in order to characterize wide-knit pantographic structures more precisely, a criterion referred to as wide-knit ratio is defined as follows

$$\omega = \frac{n_f \lambda}{\ell} = \frac{n_f (a\sqrt{2})}{\ell} \tag{8}$$

where n_f is the number of fibers of one of the two families attached to the short side, ℓ the length of the short side, and a is the depth of the fiber cross section (see Fig. 2). This ratio ω clearly lies within the range $\omega \in (0, 1]$, where, when the upper limit value is reached, then we are considering a grid which is very similar to a plate.

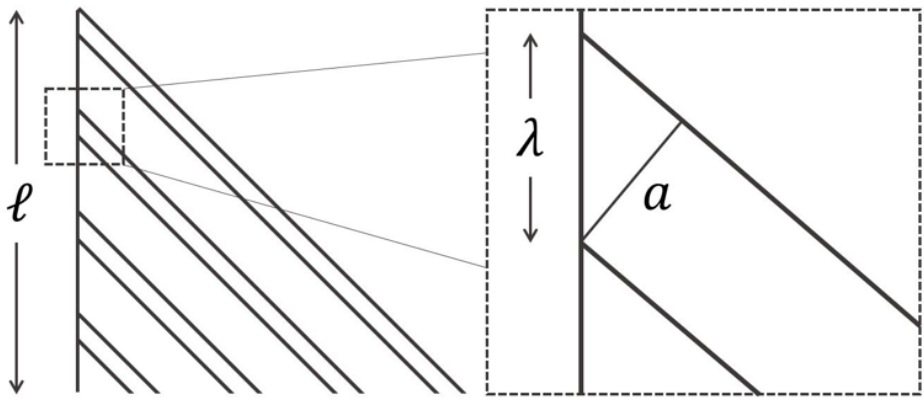

Figure 2. Schematic representation of the dimensions involved in the computation of the wide-knit ratio ω.

The used numerical code has been implemented with a standard package available in COMSOL Multiphysics®, namely, Weak Form PDE. In Weak Form PDE package, energy terms are introduced along with defined dependent variables (two placement fields in this study), and a tensorial field, which is constrained to be equal to the gradient of placement fields (by using the method of Lagrangian multipliers), is defined so that energy expressions requiring a second gradient of placements are easily introduced[36].

3 Comparison of numerical simulations with experimental measurements

In this section, by using the model detailed in the previous section, numerical predictions are presented for the wide-knit pantographic layer under study and compared with experimental measures. A 3D-printed wide-knit pantographic layer with the length, $L = 210$ mm, and height, $\ell = 70$ mm, is considered in this study. The wide-knit ratio of the structure is about 0.09, which indicates a quite low fiber density. Fibers have a rectangular cross section with $a = 0.9$ mm and $b = 1.6$ mm, where a and b are the height and width of the cross section, respectively. Also, the two families of fibers are interconnected with pivots with a radius of 0.5 mm. The wide-knit pantographic layer is made of polyamide PA 2200, whose Young's modulus is $Y_p = 1600$ MPa, and the Poisson's ratio is $\nu = 0.36$. In the numerical simulations, the prescribed displacement boundary condition is applied at one of the short sides to simulate a bias extension test while the other short side is kept fixed. The following constitutive parameters

are used in the numerical simulations: $K_e = 1.86 \times 10^5\,\mathrm{N/m}$, $K_b = 1.26 \times 10^{-2}\,\mathrm{Nm}$, $K_p = 30\,\mathrm{N/m}$, and $K_f = 8 \times 10^6\,\mathrm{N/m^3}$.

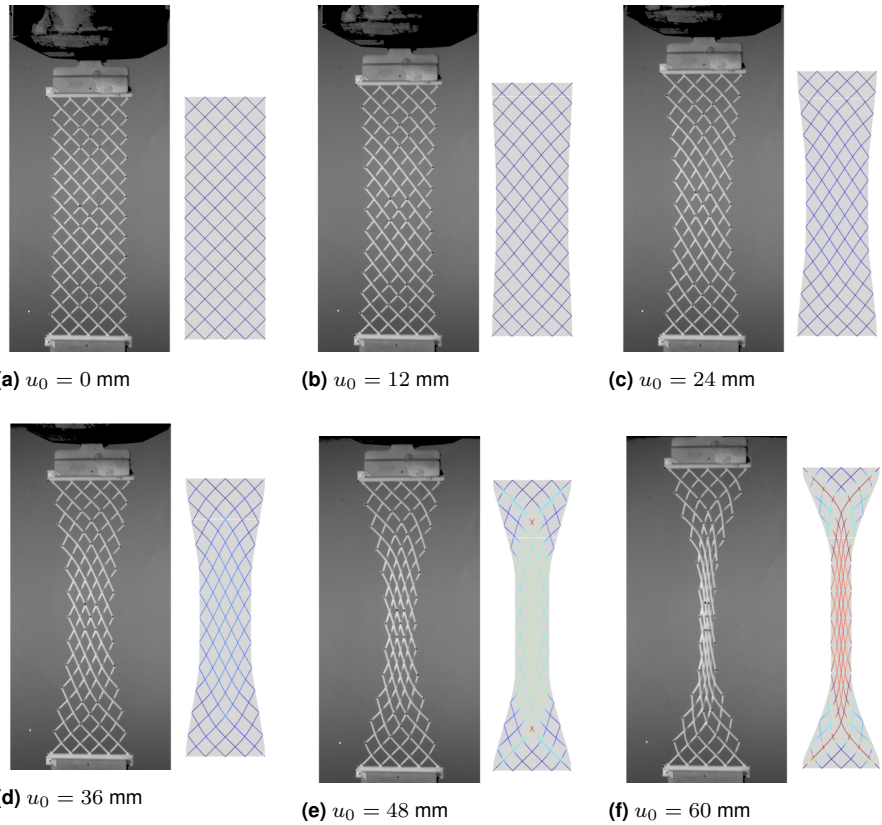

(a) $u_0 = 0$ mm **(b)** $u_0 = 12$ mm **(c)** $u_0 = 24$ mm

(d) $u_0 = 36$ mm **(e)** $u_0 = 48$ mm **(f)** $u_0 = 60$ mm

Figure 3. Comparison between experimental measurements and numerical simulations under bias extension test

The experimental measurements and theoretical predictions are compared during extension of the wide-knit pantographic structure under study in Fig. 3. The figures (see Figs. 3a-3f) are provided for different values of prescribed displacement, namely for $u_0 = 0, 12, 24, 36, 48$, and 60 mm, respectively. As it can be seen by comparison, numerical results match perfectly the experimental measures. In order to have a better interpretation of the theoretical predictions, two sets of material lines have been assigned in the second-gradient continua, which are oriented exactly along the directions of fibers. In this way, it is shown how the second-gradient model can be effectively applied to investigate the mechanical behavior of wide-knit pantographic structures.

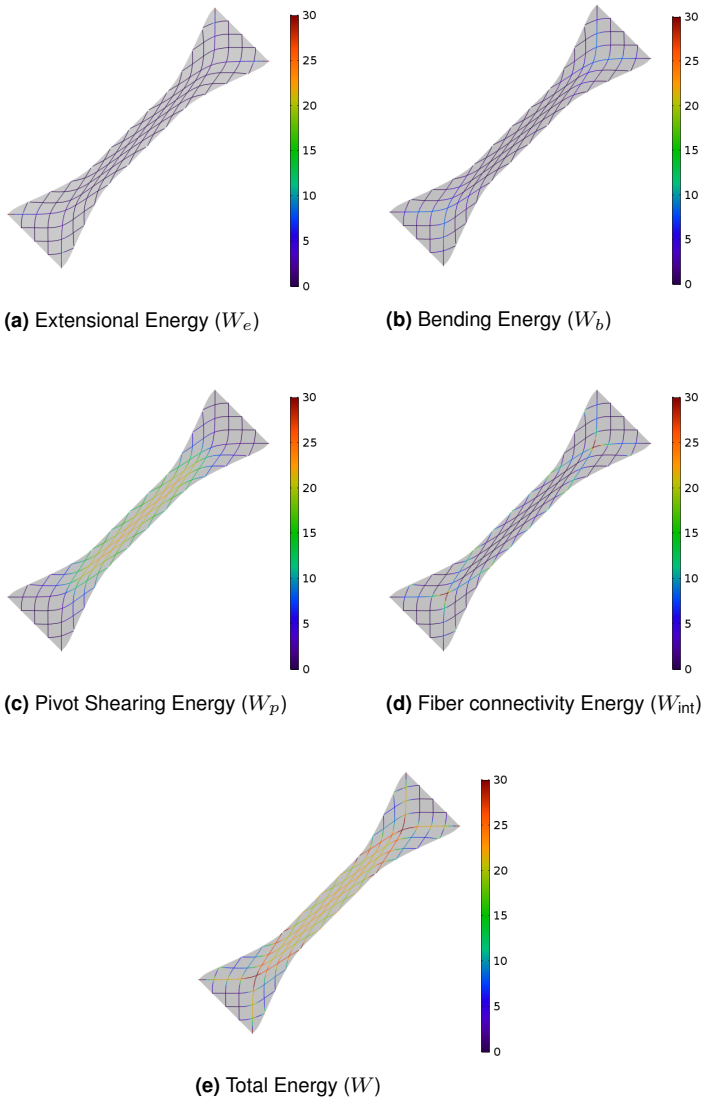

(a) Extensional Energy (W_e)

(b) Bending Energy (W_b)

(c) Pivot Shearing Energy (W_p)

(d) Fiber connectivity Energy (W_{int})

(e) Total Energy (W)

Figure 4. Contribution of energy terms.

As it is seen in Fig. 3, the behaviors of fibers in the experiment and material lines in the simulation are quite similar to each other. Additionally, contributions of the energy terms given in the total deformation energy expression are investigated in Fig. 4. Each term is plotted for the particular value of prescribed displacement, $u_0 = 60$ mm. As it can be observed in Fig. 4, pivots have a substantial role in the overall mechanical behavior of the structure. The shear energy is considerably large in the center of the specimen while fiber

connectivity energy is high around the intersections of the fibers connected to both lower and upper corners of the specimen. On the other hand, the terms related to extension and bending are slightly large at both ends of the specimen, especially on the fibers connected at the corners of the pantographic structure. It is clear that in the center of the specimen energy terms due to the existence of pivots are dominant.

In order to give a better insight on pivot behavior during the extension test, distance between two families of fibers $\|\boldsymbol{\chi}^1 - \boldsymbol{\chi}^2\|$ is plotted in Fig. 5 for a selected value of the prescribed displacement, namely $u_0 = 60$ mm. As it can be seen in Fig. 5, relative distances on the fibers connected to the corners of the specimen are large. Indeed, this indicates that failure of the structure may potentially occur on these fibers.

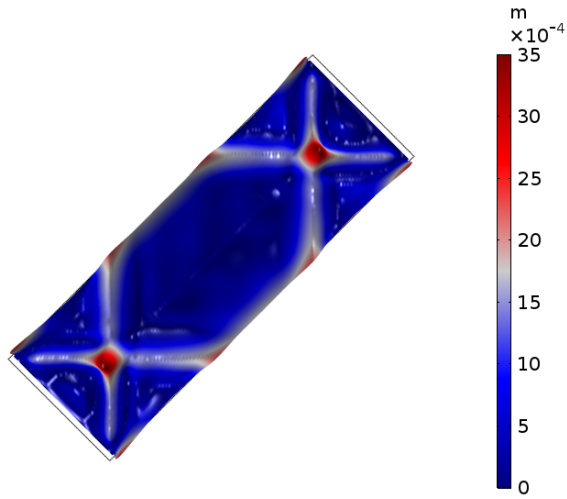

Figure 5. Relative displacement between two families of fibers.

Moreover, force-displacement plots of the experiment and simulation are compared in Fig. 6. In the experiment, it is observed that pivots may get broken when large displacements occur. As it is shown in Fig. 6, some minor jumps are observed around 60 mm of displacement. Then, the experimental plot, at around 64.4 mm of displacement, has an abrupt jump: at this point, as it is shown in Fig. 7, three pivots got broken in the lower part of the specimen. The damage occurs around the intersection of the fibers connected at the lower corners of the specimen. Overall, the numerically obtained force-displacement plot compares very well with those experimentally measured .

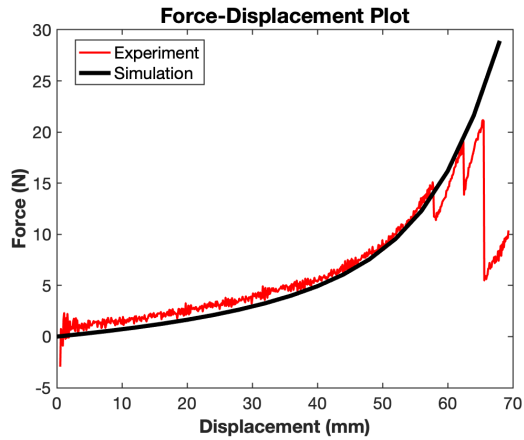

Figure 6. Force-Displacement Plot (Experiment vs Simulation).

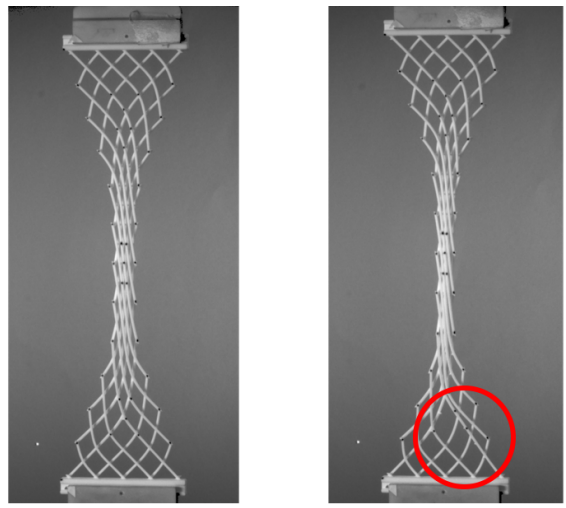

Figure 7. Pivot damage observed during bias extension test.

4 Conclusions

In this work, inspired by the pioneering works of P. Germain[11], Mindlin[10], Toupin[14] and Sedov[37] on second gradient theories, we have shown that it is natural to model the mechanical response of pantographic structures with a continuous second gradient model even when the fibers of these structures are not dense enough to justify the use of

a continuous theory (which, instead, seems to be the natural choice when dealing with dense knitted fabrics).

The fundamental point proposed in this paper was to show that the presence of a microstructure, or better an architecture, in some cases make it possible to use models where the strain energy depends not only on the gradient of the displacement, but also on its second gradient, even when microstructure cannot actually be considered at a deeper scale of observation, as it is the case in the usual microstructured continua.

The concept of interpreting mechanical effects of microstructure by using a second gradient continuum is already a fascinating idea but it acquires greater importance when one considers a microstructure producing such effects even with few elementary cells. It should be now clear that such a structure, which can be considered as the corresponding homogenized metamaterial (even when one is very far from having a dense knitting), really exhibits high-performance mechanical properties. In the different fields of applications, it could be useful to consider the coupling with other kind of materials (e.g. granular materials[38–44], laminated plates[45–49], and micropolar materials[50–52]).

The study presented here can be completed by an analysis of the damage in pantographic structures. General discussions to investigate the damage in higher gradient theories can be found in[53–56]. Problems related to modeling and simulation of metamaterials like those presented in this paper can be greatly simplified by the introduction of appropriate numerical tools[57–72]. Finally, the problem which has been briefly presented in this article can be investigated and many of its applications can be designed and tested. This requires accurate theoretical analyses: in the literature several points of reference can be found[73–79].

References

1. M. E. Yildizdag, C. A. Tran, E. Barchiesi, M. Spagnuolo, F. dell?Isola, and F. Hild, “A multi-disciplinary approach for mechanical metamaterial synthesis: A hierarchical modular multiscale cellular structure paradigm,” in *State of the Art and Future Trends in Material Modeling*, pp. 485–505, Springer, 2019.
2. E. Barchiesi, M. Spagnuolo, and L. Placidi, “Mechanical metamaterials: a state of the art,” *Mathematics and Mechanics of Solids*, vol. 24, no. 1, pp. 212–234, 2019.
3. F. dell’Isola, P. Seppecher, M. Spagnuolo, E. Barchiesi, F. Hild, T. Lekszycki, I. Giorgio, L. Placidi, U. Andreaus, M. Cuomo, *et al.*, “Advances in pantographic structures: design, manufacturing, models, experiments and image analyses,” *Continuum Mechanics and Thermodynamics*, vol. 31, no. 4, pp. 1231–1282, 2019.
4. G. Maier, U. Perego, U. Andreaus, R. Esposito, S. Forest, *et al.*, “The Complete Works of Gabrio Piola: Volume I Commented English Translation-English and Italian Edition,” 2014.
5. F. dell’ÄôIsola, U. Andreaus, A. Cazzani, R. Esposito, L. Placidi, U. Perego, G. Maier, and P. Seppecher, “The Complete Works of Gabrio Piola: Volume II,” 2014.
6. N. Auffray, F. dell’Isola, V. Eremeyev, A. Madeo, and G. Rosi, “Analytical continuum mechanics à la Hamilton–Piola least action principle for second gradient continua and capillary fluids,” *Mathematics and Mechanics of Solids*, vol. 20, no. 4, pp. 375–417, 2015.

7. Y. Rahali, I. Giorgio, J. Ganghoffer, and F. dell'Isola, "Homogenization à la Piola produces second gradient continuum models for linear pantographic lattices," *International Journal of Engineering Science*, vol. 97, pp. 148–172, 2015.
8. F. dell'Isola, A. Della Corte, R. Esposito, and L. Russo, "Some cases of unrecognized transmission of scientific knowledge: from antiquity to Gabrio Piola'Äôs peridynamics and generalized continuum theories," in *Generalized continua as models for classical and advanced materials*, pp. 77–128, Springer, 2016.
9. F. dell'Isola, A. Della Corte, and I. Giorgio, "Higher-gradient continua: The legacy of Piola, Mindlin, Sedov and Toupin and some future research perspectives," *Mathematics and Mechanics of Solids*, p. 1081286515616034, 2016.
10. R. D. Mindlin and N. N. Eshel, "On first strain-gradient theories in linear elasticity," *International Journal of Solids and Structures*, vol. 4, no. 1, pp. 109–124, 1968.
11. P. Germain, "The method of virtual power in continuum mechanics. part 2: Microstructure," *SIAM Journal on Applied Mathematics*, vol. 25, no. 3, pp. 556–575, 1973.
12. S. Atluri and A. Cazzani, "Rotations in computational solid mechanics," *Archives of Computational Methods in Engineering*, vol. 2, no. 1, pp. 49–138, 1995.
13. A. Cazzani and S. Atluri, "Four-noded mixed finite elements, using unsymmetric stresses, for linear analysis of membranes," *Computational Mechanics*, vol. 11, no. 4, pp. 229–251, 1993.
14. R. A. Toupin, "Theories of elasticity with couple-stress," 1964.
15. A. C. Eringen, "Mechanics of micromorphic continua," in *Mechanics of generalized continua*, pp. 18–35, Springer, 1968.
16. A. Misra and P. Poorsolhjouy, "Elastic behavior of 2D grain packing modeled as micromorphic media based on granular micromechanics," *Journal of Engineering Mechanics*, vol. 143, no. 1, p. C4016005, 2017.
17. V. A. Eremeyev, "On the characterization of the nonlinear reduced micromorphic continuum with the local material symmetry group," in *Higher Gradient Materials and Related Generalized Continua*, pp. 43–54, Springer, 2019.
18. Y. Solyaev, S. Lurie, E. Barchiesi, and L. Placidi, "On the dependence of standard and gradient elastic material constants on a field of defects," *Mathematics and Mechanics of Solids*, vol. 25, no. 1, pp. 35–45, 2020.
19. J.-J. Alibert, P. Seppecher, and F. dell'Isola, "Truss modular beams with deformation energy depending on higher displacement gradients," *Mathematics and Mechanics of Solids*, vol. 8, no. 1, pp. 51–73, 2003.
20. F. dell'Isola, I. Giorgio, M. Pawlikowski, and N. Rizzi, "Large deformations of planar extensible beams and pantographic lattices: heuristic homogenization, experimental and numerical examples of equilibrium," *Proc. R. Soc. A*, vol. 472, no. 2185, p. 20150790, 2016.
21. L. Placidi, U. Andreaus, and I. Giorgio, "Identification of two-dimensional pantographic structure via a linear d4 orthotropic second gradient elastic model," *Journal of Engineering Mathematics*, vol. 103, no. 1, pp. 1–21, 2017.
22. L. Placidi, E. Barchiesi, E. Turco, and N. L. Rizzi, "A review on 2D models for the description of pantographic fabrics," *Zeitschrift für Angewandte Mathematik und Physik*, vol. 67, no. 5, p. 121, 2016.
23. D. Scerrato, I. Giorgio, and N. L. Rizzi, "Three-dimensional instabilities of pantographic sheets with parabolic lattices: numerical investigations," *Zeitschrift für Angewandte*

Mathematik und Physik, vol. 67, no. 3, p. 53, 2016.
24. I. Giorgio, N. Rizzi, and E. Turco, "Continuum modelling of pantographic sheets for out-of-plane bifurcation and vibrational analysis," *Proc. R. Soc. A*, vol. 473, no. 2207, p. 20170636, 2017.
25. V. A. Eremeyev, F. dell'Isola, C. Boutin, and D. Steigmann, "Linear pantographic sheets: existence and uniqueness of weak solutions," *Journal of Elasticity*, pp. 1–22, 2017.
26. D. Scerrato and I. Giorgio, "Equilibrium of two-dimensional cycloidal pantographic metamaterials in three-dimensional deformations," *Symmetry*, vol. 11, no. 12, p. 1523, 2019.
27. U. Andreaus, M. Spagnuolo, T. Lekszycki, and S. R. Eugster, "A Ritz approach for the static analysis of planar pantographic structures modeled with nonlinear Euler–Bernoulli beams," *Continuum Mechanics and Thermodynamics*, pp. 1–21, 2018.
28. P. Harrison, "Modelling the forming mechanics of engineering fabrics using a mutually constrained pantographic beam and membrane mesh," *Composites Part A: Applied Science and Manufacturing*, vol. 81, pp. 145–157, 2016.
29. J. Alibert and A. Della Corte, "Second-gradient continua as homogenized limit of pantographic microstructured plates: a rigorous proof," *Zeitschrift für Angewandte Mathematik und Physik*, vol. 66, no. 5, pp. 2855–2870, 2015.
30. C. Boutin, I. Giorgio, L. Placidi, *et al.*, "Linear pantographic sheets: Asymptotic micro-macro models identification," *Mathematics and Mechanics of Complex Systems*, vol. 5, no. 2, pp. 127–162, 2017.
31. I. Giorgio, "Numerical identification procedure between a micro-Cauchy model and a macro-second gradient model for planar pantographic structures," *Zeitschrift für Angewandte Mathematik und Physik*, vol. 67(4), no. 95, 2016.
32. I. Giorgio, F. dell'Isola, and D. Steigmann, "Axisymmetric deformations of a 2nd grade elastic cylinder," *Mechanics Research Communications*, vol. 94, pp. 45–48, 2018.
33. I. Giorgio, P. Harrison, F. dell'Isola, J. Alsayednoor, and E. Turco, "Wrinkling in engineering fabrics: a comparison between two different comprehensive modelling approaches," *Proceedings of the Royal Society A: Mathematical, Physical and Engineering Sciences*, vol. 474, no. 2216, p. 20180063, 2018.
34. E. Turco, I. Giorgio, A. Misra, and F. dell'Isola, "King post truss as a motif for internal structure of (meta) material with controlled elastic properties," *Royal Society open science*, vol. 4, no. 10, p. 171153, 2017.
35. M. Spagnuolo, K. Barcz, A. Pfaff, F. dell'Isola, and P. Franciosi, "Qualitative pivot damage analysis in aluminum printed pantographic sheets: Numerics and experiments," *Mechanics Research Communications*, vol. 83, pp. 47–52, 2017.
36. D. Scerrato, I. A. Zhurba Eremeeva, T. Lekszycki, and N. L. Rizzi, "On the effect of shear stiffness on the plane deformation of linear second gradient pantographic sheets," *ZAMM-Journal of Applied Mathematics and Mechanics/Zeitschrift für Angewandte Mathematik und Mechanik*, vol. 96, no. 11, pp. 1268–1279, 2016.
37. L. I. Sedov, "Mathematical methods for constructing new models of continuous media," *Russian Mathematical Surveys*, vol. 20, no. 5, p. 123, 1965.
38. H. Jia, A. Misra, P. Poorsolhjouy, and C. Liu, "Optimal structural topology of materials with micro-scale tension-compression asymmetry simulated using granular micromechanics," *Materials & Design*, vol. 115, pp. 422–432, 2017.

39. A. Misra and P. Poorsolhjouy, "Grain-and macro-scale kinematics for granular micromechanics based small deformation micromorphic continuum model," *Mechanics Research Communications*, vol. 81, pp. 1–6, 2017.
40. E. Turco, "In-plane shear loading of granular membranes modeled as a Lagrangian assembly of rotating elastic particles," *Mechanics Research Communications*, vol. 92, pp. 61–66, 2018.
41. E. Turco, F. dell'Isola, and A. Misra, "A nonlinear Lagrangian particle model for grains assemblies including grain relative rotations," *International Journal for Numerical and Analytical Methods in Geomechanics*, vol. 43, no. 5, pp. 1051–1079, 2019.
42. A. Bilotta, A. Morassi, E. Rosset, E. Turco, and S. Vessella, "Numerical size estimates of inclusions in Kirchhoff–Love elastic plates," *International Journal of Solids and Structures*, vol. 168, pp. 58–72, 2019.
43. A. Misra and P. Poorsolhjouy, "Granular micromechanics model for damage and plasticity of cementitious materials based upon thermomechanics," *Mathematics and Mechanics of Solids*, p. 1081286515576821, 2015.
44. V. A. Eremeyev, "On the material symmetry group for micromorphic media with applications to granular materials," *Mechanics Research Communications*, vol. 94, pp. 8–12, 2018.
45. A. Cazzani, M. Serra, F. Stochino, and E. Turco, "A refined assumed strain finite element model for statics and dynamics of laminated plates," *Continuum Mechanics and Thermodynamics*, pp. 1–28.
46. H. Altenbach, V. A. Eremeyev, and K. Naumenko, "On the use of the first order shear deformation plate theory for the analysis of three-layer plates with thin soft core layer," *ZAMM-Journal of Applied Mathematics and Mechanics/Zeitschrift für Angewandte Mathematik und Mechanik*, vol. 95, no. 10, pp. 1004–1011, 2015.
47. H. Altenbach and V. A. Eremeyev, "Thin-walled structures made of foams," in *Cellular and Porous Materials in Structures and Processes*, pp. 167–242, Springer, 2010.
48. H. Altenbach and V. A. Eremeyev, "Direct approach-based analysis of plates composed of functionally graded materials," *Archive of Applied Mechanics*, vol. 78, no. 10, pp. 775–794, 2008.
49. H. Altenbach and V. A. Eremeyev, "On the bending of viscoelastic plates made of polymer foams," *Acta Mechanica*, vol. 204, no. 3-4, p. 137, 2009.
50. W. Pietraszkiewicz and V. Eremeyev, "On natural strain measures of the non-linear micropolar continuum," *International Journal of Solids and Structures*, vol. 46, no. 3, pp. 774–787, 2009.
51. H. Altenbach and V. Eremeyev, "On the linear theory of micropolar plates," *ZAMM-Journal of Applied Mathematics and Mechanics/Zeitschrift für Angewandte Mathematik und Mechanik*, vol. 89, no. 4, pp. 242–256, 2009.
52. V. A. Eremeyev and W. Pietraszkiewicz, "Material symmetry group and constitutive equations of micropolar anisotropic elastic solids," *Mathematics and Mechanics of Solids*, vol. 21, no. 2, pp. 210–221, 2016.
53. L. Placidi and E. Barchiesi, "Energy approach to brittle fracture in strain-gradient modelling," *Proc. R. Soc. A*, vol. 474, no. 2210, p. 20170878, 2018.
54. L. Placidi, A. Misra, and E. Barchiesi, "Two-dimensional strain gradient damage modeling: a variational approach," *Zeitschrift für Angewandte Mathematik und Physik*, vol. 69, no. 3, p. 56, 2018.

55. L. Placidi, E. Barchiesi, and A. Misra, "A strain gradient variational approach to damage: a comparison with damage gradient models and numerical results," *Mathematics and Mechanics of Complex Systems*, vol. 6, no. 2, pp. 77–100, 2018.
56. L. Placidi, A. Misra, and E. Barchiesi, "Simulation results for damage with evolving microstructure and growing strain gradient moduli," *Continuum Mechanics and Thermodynamics*, pp. 1–21, 2018.
57. A. Cazzani, F. Stochino, and E. Turco, "An analytical assessment of finite element and isogeometric analyses of the whole spectrum of Timoshenko beams," *ZAMM-Journal of Applied Mathematics and Mechanics/Zeitschrift für Angewandte Mathematik und Mechanik*, vol. 96, no. 10, pp. 1220–1244, 2016.
58. A. Cazzani, M. Malagù, and E. Turco, "Isogeometric analysis: a powerful numerical tool for the elastic analysis of historical masonry arches," *Continuum Mechanics and Thermodynamics*, vol. 28, no. 1-2, pp. 139–156, 2016.
59. A. Cazzani, M. Malagù, E. Turco, and F. Stochino, "Constitutive models for strongly curved beams in the frame of isogeometric analysis," *Mathematics and Mechanics of Solids*, vol. 21, no. 2, pp. 182–209, 2016.
60. A. Cazzani, M. Malagù, and E. Turco, "Isogeometric analysis of plane-curved beams," *Mathematics and Mechanics of Solids*, vol. 21, no. 5, pp. 562–577, 2016.
61. A. Luongo, D. Zulli, and G. Piccardo, "Analytical and numerical approaches to nonlinear galloping of internally resonant suspended cables," *Journal of Sound and Vibration*, vol. 315, no. 3, pp. 375–393, 2008.
62. L. Placidi, E. Barchiesi, and A. Battista, "An inverse method to get further analytical solutions for a class of metamaterials aimed to validate numerical integrations," in *Mathematical Modelling in Solid Mechanics*, pp. 193–210, Springer, 2017.
63. L. Greco, M. Cuomo, and L. Contrafatto, "Two new triangular g1-conforming finite elements with cubic edge rotation for the analysis of kirchhoff plates," *Computer Methods in Applied Mechanics and Engineering*, vol. 356, pp. 354–386, 2019.
64. L. Greco, M. Cuomo, and L. Contrafatto, "A quadrilateral G1-conforming finite element for the Kirchhoff plate model," *Computer Methods in Applied Mechanics and Engineering*, vol. 346, pp. 913–951, 2019.
65. L. Greco and M. Cuomo, "B-Spline interpolation of Kirchhoff-Love space rods," *Computer Methods in Applied Mechanics and Engineering*, vol. 256, pp. 251–269, 2013.
66. M. Cuomo, L. Contrafatto, and L. Greco, "A variational model based on isogeometric interpolation for the analysis of cracked bodies," *International Journal of Engineering Science*, vol. 80, pp. 173–188, 2014.
67. L. Beirão Da Veiga, T. Hughes, J. Kiendl, C. Lovadina, J. Niiranen, A. Reali, and H. Speleers, "A locking-free model for Reissner–Mindlin plates: Analysis and isogeometric implementation via NURBS and triangular NURPS," *Mathematical Models and Methods in Applied Sciences*, vol. 25, no. 08, pp. 1519–1551, 2015.
68. J. Niiranen, V. Balobanov, J. Kiendl, and S. Hosseini, "Variational formulations, model comparisons and numerical methods for Euler–Bernoulli micro-and nano-beam models," *Mathematics and Mechanics of Solids*, vol. 24, no. 1, pp. 312–335, 2019.
69. V. Balobanov and J. Niiranen, "Locking-free variational formulations and isogeometric analysis for the Timoshenko beam models of strain gradient and classical elasticity," *Computer*

Methods in Applied Mechanics and Engineering, vol. 339, pp. 137–159, 2018.
70. M. E. Yildizdag, I. T. Ardic, M. Demirtas, and A. Ergin, "Hydroelastic vibration analysis of plates partially submerged in fluid with an isogeometric FE-BE approach," *Ocean Engineering*, vol. 172, pp. 316–329, 2019.
71. M. E. Yildizdag, I. T. Ardic, A. Kefal, and A. Ergin, "An isogeometric FE-BE method and experimental investigation for the hydroelastic analysis of a horizontal circular cylindrical shell partially filled with fluid," *Thin-Walled Structures*, vol. 151, p. 106755, 2020.
72. L. Greco, "An iso-parametric g1-conforming finite element for the nonlinear analysis of kirchhoff rod. part i: the 2d case," *Continuum Mechanics and Thermodynamics*, pp. 1–24, 2020.
73. C. Pideri and P. Seppecher, "A second gradient material resulting from the homogenization of an heterogeneous linear elastic medium," *Continuum Mechanics and Thermodynamics*, vol. 9, no. 5, pp. 241–257, 1997.
74. M. Camar-Eddine and P. Seppecher, "Determination of the closure of the set of elasticity functionals," *Archive for Rational Mechanics and Analysis*, vol. 170, no. 3, pp. 211–245, 2003.
75. M. Camar-Eddine and P. Seppecher, "Non-local interactions resulting from the homogenization of a linear diffusive medium," *Comptes Rendus de l'Académie des Sciences-Series I-Mathematics*, vol. 332, no. 5, pp. 485–490, 2001.
76. G. Bouchitté, O. Mattei, G. W. Milton, and P. Seppecher, "On the forces that cable webs under tension can support and how to design cable webs to channel stresses," *Proceedings of the Royal Society A*, vol. 475, no. 2223, p. 20180781, 2019.
77. P. Seppecher, "Moving contact lines in the Cahn-Hilliard theory," *International Journal of Engineering Science*, vol. 34, no. 9, pp. 977–992, 1996.
78. S. Eugster, C. Hesch, P. Betsch, and C. Glocker, "Director-based beam finite elements relying on the geometrically exact beam theory formulated in skew coordinates," *International Journal for Numerical Methods in Engineering*, vol. 97, no. 2, pp. 111–129, 2014.
79. S. Eugster, D. Steigmann, *et al.*, "Continuum theory for mechanical metamaterials with a cubic lattice substructure," *Mathematics and Mechanics of Complex Systems*, vol. 7, no. 1, pp. 75–98, 2019.